PROPAGATION OF TRANSIENT WAVES THROUGH A STRATIFIED FLUID MEDIUM: WAVELET ANALYSIS OF A NONASYMPTOTIC DECOMPOSITION OF THE PROPAGATOR . Part 1. SPHERICAL WAVES THROUGH A TWO-LAYERED SYSTEM

Ginette Saracco

Propagation of transient waves through a stratified fluid medium: Wavelet analysis of a nonasymptotic decomposition of the propagator. Part I. Spherical waves through a two-layered system

G. Saracco[a),b)]
C.N.R.S., Laboratoire de Mécanique et d'Acoustique, Equipe Ultrasons, 31 Ch. J. Aiguier, 13402 Marseille Cedex 09, France

(Received 27 February 1991; revised 28 March 1993; accepted 20 September 1993)

The propagator for the problem of transient waves in a stratified fluid medium has a natural decomposition into three contributions. These contributions are studied in detail by analytic and numerical methods and the results are compared with experiment. Since the individual contributions have dispersive character, they are analyzed with the help of continuous wavelet transforms.

PACS numbers: 43.20.Bi, 43.20.Fn, 43.20.Hq, 43.30.Dr

INTRODUCTION

This paper deals with the propagation of transient waves through a stratified fluid medium in three dimensions. We suppose that the properties of the medium (sound velocity and density) depend on the depth only. The source is located in the medium with lower velocity. Our main concern is the definition, description, and calculation of "interface" contributions for transient sources.

(1) In order to motivate our approach, we start with a discussion of known results, which have been obtained in a somewhat different context.

For the case of a monochromatic source this problem has been extensively studied.[1-11] The interface contribution, called "lateral wave" has been examined theoretically by Gerjuoy, Brekhovskikh, and others. This wave contribution appears—as a correction to geometrical acoustics—in the estimation of the reflected acoustic potential with the help of the steepest descent method, in the asymptotic limit where the dimensionless parameter $\omega R/c$ is large. (Here, ω is the circular frequency, R is the distance between the source and the observation point, and c is the propagation velocity in the medium containing the source.)

The same methods apply to the transmitted field, where however the physical behavior is different. Here the lateral contribution is predominant in subcritical transmission, i.e., under conditions of total reflection. ("Total reflection" is a term of geometrical acoustics, which is here only the asymptotic limit.) The amplitude of the lateral contribution is an exponentially decreasing function of depth and depends on frequency. Consequently, for nonharmonic sources, it gives rise to an effective dispersion.[11-13]

The above statements have been confirmed by numerical and experimental work. In particular, it was possible to separate experimentally the various contributions (in an acoustic tank, for the air–water interface), and to show that—for audible frequencies between 3 and 5 kHz—the lateral contribution is not negligible in some regions, in agreement with numerical evaluations of the pressure field.[12]

This contribution corresponds to the echo gallery wave (whispering wave), that appears in problems of scattering in curved fluid–solid interfaces (e.g., spheres).[13,14]

(2) We come now to the case of a transient source (arbitrary time dependence). The consideration of such sources is often necessary for experimental reasons. For instance, in the study of propagation of audible signals it is often necessary to emit short wave trains in order to avoid spurious effects due to reflections on walls. Furthermore, the study of time-dependent sources is necessary in order to convert the dispersive properties of surface contributions into time delays.

It then becomes necessary to define appropriately the various contributions in transient situations, to calculate them precisely, and to study their importance in comparison to the classical geometric waves. This is the main aim of this paper.

There exist many methods for analyzing transient signals. Most works combine classical numerical methods with either a Fourier transform[15-17] or with a spectral analysis of a differential self-adjoint operator[18,19] or with the Cagniard–De Hoop method.[20-22] Some use numerical methods based on fourth-order finite-difference schemes in time and space.[23] If we want to make an exact calculation of the different contributions of the field while staying close to the physics of the phenomena, we must use a linear time-frequency or time-scale method. One class of such methods, the wavelet transforms,[24-28] has been used recently with success in several domains. The signal is decomposed into a basis of functions well localized simultaneously in time and frequency. This transform is nonparametric. The total energy of the signal is preserved.

(3) The main points of this paper are the following:

(a) The Green's function $G(x,y,z,t)$ for our problem has a standard integral representation, given below, in (4).

[a)]Present address: Penn State University, Applied Research Laboratory, P.O. Box 30, State College, PA 16804.
[b)]New address: Geosciences—Rennes I, Laboratoire de Geophysique Interne, Bâtiment 15, Campus de Beaulieu, 35042 Rennes Cedex, France.

Consequently G can be decomposed into its three natural contributions corresponding to intervals between branch points in an integrand, and given below, in (5)–(7). They give rise to different "propagation modes." By analogy with the monochromatic case,[11,12] we call them "geometric," "surface," and "evanescent" or "third" contribution.

We want to stress the fact that this decomposition is valid in general, and does not depend on any assumption of asymptotic nature. This means that our use of the word "geometric" can be misleading. For this reason, we keep it in quotes.

The same decomposition holds for a solution with an arbitrary source, which is discussed in Sec. I.

(b) The individual contributions are of "dispersive nature," i.e., their effective propagation velocity depends on frequency. It is convenient to analyze such functions through continuous wavelet transforms, and in Sec. III we shall perform such an analysis. By using the properties of the analyzing wavelet (regularity and progressivity) and general properties of the wavelet transform (isometry and linearity) we obtain methods for numerical computation of each contribution. These methods are precise and robust due to the "regularizing" properties of the wavelet transform. The transform of the Green's function is more regular than the Green's function itself,[29,30] but still allows a precise localization of various wave fronts, and selective reconstruction of the pressure field.

I. DECOMPOSITION OF ACOUSTIC POTENTIALS INTO THREE CONTRIBUTIONS

The problem is three-dimensional in space. There are two fluid media separated by a plane interface $z=0$. The first two spatial variables are written as $\mathbf{r}=(x,y)$. The medium of lower velocity c_1 is the half-space $z<0$ and contains a source $s(\mathbf{r},z,t)$. It is convenient to consider a whole family of such sources $s(\mathbf{r},z-h,t)$, labeled by a "height parameter" h, where h varies in a suitable interval. We assume the following:

(i) s is a product: $s(\mathbf{r},z-h,t)=F(t)Q(\mathbf{r},z-h)$, where F and Q are real.

(ii) For each $z,h,Q(\mathbf{r},z-h)$ is radially symmetric, i.e., depends only on $r=|\mathbf{r}|$.

(iii) $Q(\mathbf{r},z-h)=0$ for $z>0$ and for all h in the interval that we consider.

(iv) The source vanishes if t is negative or larger than some T. $F(t)=0$ if $t\leqslant 0$, or if $t\geqslant T$ $(T>0)$.

We define the Fourier transform with respect to the first two spatial variables $\mathbf{r}=(x,y)$ and the time variable t as:

$$\hat{\Phi}(\mu,z,\omega)=\frac{1}{4\pi^2\sqrt{2\pi}}\int\int \Phi(\mathbf{r},z,t)e^{i(\omega t-\mu r)}\,d\mathbf{r}\,d\omega.$$

In order to keep the notations simple, we shall use the same notation for the Fourier transform with respect to the variable $\mathbf{r}$ only

$$\hat{\Phi}(\mu,z,t)=\frac{1}{4\pi^2}\int \Phi(\mathbf{r},z,t)e^{-i\mu r}\,d\mathbf{r}.$$

Similarly,

$$\hat{\Phi}(\mathbf{r},z,\omega)=\frac{1}{\sqrt{2\pi}}\int \Phi(\mathbf{r},z,t)e^{i\omega t}\,d\omega.$$

If Φ is radially symmetric, it can be written in terms of $\hat{\Phi}$ as

$$\Phi(r,z,t)=\sqrt{2\pi}\int_{\omega=-\infty}^{\infty}e^{-i\omega t}\int_{\mu=0}^{\infty}\hat{\Phi}(\mu,z,\omega)\times J_0(\mu r)\mu\,d\mu\,d\omega,$$

where $\mu=|\mu|$ and J_0 is the Bessel function of order zero.

The propagation will be described in terms of the scalar acoustic potential Ψ. Let us write:

$$D\Psi=\frac{\partial\Psi}{\partial t},\quad \nabla\Psi=\left(\frac{\partial\Psi}{\partial x},\frac{\partial\Psi}{\partial y},\frac{\partial\Psi}{\partial z}\right).$$

The wave equation in a stratified fluid medium in which the velocity (c) and the density (ρ) depend on only one spatial variable—the depth z—and are piecewise constant, can be written as[18,19]

$$\rho(z)\nabla\cdot\left(\frac{1}{\rho(z)}\nabla\Psi\right)-c^{-2}(z)D^2\Psi=-s(\mathbf{r},z-h,t).\quad(1)$$

The initial conditions are

$$\Psi(\mathbf{r},z,0)=0,\quad D\Psi(\mathbf{r},z,0)=0.$$

The problem is to find Ψ satisfying the two above conditions, the classical boundary conditions for fluid media (continuity of the pression and of the normal velocity) and such that: (i) $\Psi(r,z,t)$ is real and (ii) $\Psi(r,z,t)=0$ for $t<0$ (causality).

Taking into account a two-layered pattern, we denote by n the refraction index (ratio of celerities), $n=c_1/c_2<1$, and by m the ratio of the densities $m=\rho_2/\rho_1$, A_1 and A_2 are the coefficient of reflection and transmission.

The solution to this problem is well known (Sommerfeld and Wells) see Cagniard.[20] The acoustic potential in the two media is

$$\hat{\Psi}_1(\mu,z,\omega)=A_1(\mu,\omega)e^{-i\,\mathrm{sgn}(\omega)K_1(\mu,\omega)z}+\frac{i\,\mathrm{sgn}(\omega)\hat{F}(\omega)\hat{Q}(\mu,z)}{2\pi\sqrt{2\pi}K_1(\mu,\omega)}\times e^{i\,\mathrm{sgn}(\omega)K_1(\mu,\omega)|z+h|}\quad(z<0)$$

$$\hat{\Psi}_2(\mu,z,\omega)=A_2(\mu,\omega)e^{i\,\mathrm{sgn}(\omega)K_2(\mu,\omega)z}\quad(z>0),$$

where $K_j(\mu,\omega)=\sqrt{\omega^2/c_j^2-\mu^2}$ and $\mathrm{Im}[K_j]\geqslant 0$, for $\omega>0$, $j=1,2$ [Rk: $\mathrm{sgn}(\omega)K_j$ is continuous in $\omega=0$]. The values of the coefficients of reflection A_1 and of transmission A_2 are

$$A_1(\mu,\omega)=\frac{i\,\mathrm{sgn}(\omega)\hat{F}(\omega)\hat{Q}(\mu,z)}{2\pi\sqrt{2\pi}K_1(\omega,\mu)}\frac{[mK_1(\mu,\omega)-K_2(\mu,\omega)]}{[mK_1(\mu,\omega)+K_2(\mu,\omega)]}\times e^{i\,\mathrm{sgn}(\omega)K_1(\mu,\omega)h},$$

$$A_2(\mu,\omega)=\frac{i\,\mathrm{sgn}(\omega)\hat{F}(\omega)\hat{Q}(\mu,z)}{\pi\sqrt{2\pi}}\frac{e^{i\,\mathrm{sgn}(\omega)K_1(\mu,\omega)h}}{(mK_1(\mu,\omega)+K_2(\mu,\omega))}.$$

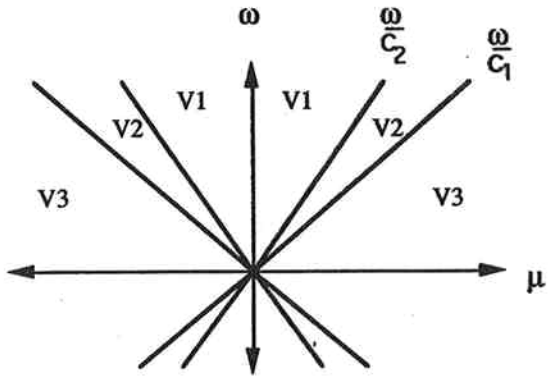

FIG. 1. Three regions in the (μ,ω) plane.

From now on, we restrict our attention to the transmitted field, and write Ψ for Ψ_2. Written out in full, it is

$$\hat{\Psi}(\mu,z,\omega)=\frac{i\,\mathrm{sgn}(\omega)\hat{F}(\omega)\hat{Q}(\mu,z)}{\pi\sqrt{2\pi}}\frac{e^{i\,\mathrm{sgn}(\omega)K_1(\mu,\omega)h}}{(mK_1(\mu,\omega)+K_2(\mu,\omega))}\times e^{i\,\mathrm{sgn}(\omega)K_2(\mu,\omega)z}. \tag{2}$$

One can verify directly that $\hat{\Psi}(\mu,z,\omega)$ and $\hat{\Psi}_1(\mu,z,\omega)$ satisfies

$$\left[\frac{\partial^2}{\partial z^2}+\left(\frac{\omega^2}{c_j^2}-\mu^2\right)\right]\hat{\Psi}_j(\mu,z,\omega)=-\hat{s}(\mu,z-h,\omega);$$

(i) $\hat{\Psi}_j(\mu,z,\omega)$ verifies the Hermitian symmetry: $\hat{\Psi}_j(\mu,z,\omega)=\hat{\Psi}_j(\mu,z,-\omega)$; (ii) $\hat{\Psi}_j(\mu,z,\omega)$ is analytic in the complex half-plane $\mathrm{Im}(\omega)>0$.

For any fixed z, the behavior of $\hat{\Psi}(\mu,z,\omega)$ depends on whether any one of the functions K_1,K_2 is real or imaginary. This distinction will be crucial in our decomposition of the acoustic potential Ψ into three contributions, corresponding to different kinds of propagation. We consider, in the μ,ω plane, the three regions V^1, V^2, V^3 (see Fig. 1):

(i) V^1: $\mu^2<\dfrac{|\omega|^2}{(c_2)^2}$ (K_1,K_2 real);

(ii) V^2: $\dfrac{|\omega|^2}{(c_2)^2}<\mu^2<\dfrac{|\omega|^2}{(c_1)^2}$ (K_1 real, K_2 imaginary);

(iii) V^3: $\dfrac{|\omega|^2}{(c_1)^2}<\mu^2$ (K_1,K_2 imaginary).

The restriction of the transmitted acoustic potential to these three regions gives a decomposition:

$$\Psi=\Psi^1+\Psi^2+\Psi^3.$$

Geometric type:

$\forall z\in R$, $\hat{\Psi}^1=\hat{\Psi}$ if $(\mu,\omega)\in V^1$, and otherwise $\hat{\Psi}^1=0$:

$$\hat{\Psi}^1(\mu,z,\omega)=\frac{i\,\mathrm{sgn}(\omega)\hat{F}(\omega)\hat{Q}(\mu,z)}{\pi\sqrt{2\pi}}\times\frac{\exp[i\,\mathrm{sgn}(\omega)\sqrt{\omega^2/c_1^2-\mu^2}h]}{(mK_1(\mu,\omega)+K_2(\mu,\omega))}\times\exp[i\,\mathrm{sgn}(\omega)\sqrt{\omega^2/c_2^2-\mu^2}z].$$

Surface type:

$\forall z\in R$, $\hat{\Psi}^2=\hat{\Psi}$ if $(\mu,\omega)\in V^2$, and otherwise $\hat{\Psi}^2=0$:

$$\hat{\Psi}^2(\mu,z,\omega)=\frac{i\,\mathrm{sgn}(\omega)\hat{F}(\omega)\hat{Q}(\mu,z)}{\pi\sqrt{2\pi}}\times\frac{\exp[i\,\mathrm{sgn}(\omega)\sqrt{\omega^2/c_1^2-\mu^2}h]}{(mK_1(\mu,\omega)+iK_2(\mu,\omega))}\times\exp(-\sqrt{\mu^2-\omega^2/c_2^2}\,z).$$

Third type:

$\forall z\in R$, $\hat{\Psi}^3=\hat{\Psi}$ if $(\mu,\omega)\in V^3$, and otherwise $\hat{\Psi}^3=0$:

$$\hat{\Psi}^3(\mu,z,\omega)=\frac{\hat{F}(\omega)\hat{Q}(\mu,z)}{\pi\sqrt{2\pi}}\frac{\exp(-\sqrt{\mu^2-\omega^2/c_1^2}h)}{(mK_1(\mu,\omega)+K_2(\mu,\omega))}\times\exp(-\sqrt{\mu^2-\omega^2/c_2^2}\,z).$$

We can remark that each of the contributions satisfies the wave equation (1), but not necessarily the causality condition. These contributions correspond to different "modes" or propagation types. We can give the following physical interpretation.

(1) The first type corresponds to geometrical acoustics. The waves corresponding to this contribution are the direct reflected or transmitted contributions corresponding to a homogeneous medium. They satisfy the classical laws of ray theory, whence the name "geometric" contributions, in analogy with the terminology of the harmonic case.

(2) The second term takes into account interface phenomena. With respect to classical ray theory, it is a correction to geometrical acoustics. In the case of a monochromatic source, it is easy to obtain an asymptotic expression for this contribution with the help of high-frequency approximations such as saddle-point or stationary-point method. They are well known, and are obtained with the help of an additional integration path around a branch point, corresponding to over-critical angles (incidence angle). However, in the transient case, these waves have essentially not been studied except experimentally. The simultaneous space and frequency dependence of the "surface" potential implies, as a consequence, the fact that these contributions can no longer be brought into correspondence with a high-frequency asymptotic expression and with a particular branch point. These contributions describe a dispersive phenomenon due to the inhomogeneity of the medium (the interface). They will be called "inhomogeneous" or "surface" contributions.

(3) The third term takes into account contributions that do not correspond to a propagation (they are rapidly

attenuated). We shall call them "evanescent" contributions. In the presence of a second interface, they become guided waves.[18]

Returning to the radial horizontal space variable r (instead of the absolute value μ of the wave vector), we have

$$\hat{\Psi}(r,z,\omega)=\frac{i\,\mathrm{sgn}(\omega)}{c_1}\sqrt{\frac{2}{\pi}}\hat{F}(\omega)|\omega|\int_{u=0}^{\infty}J_0\left(\frac{u\omega}{r}\right)\times Q(u,z)N(\omega,u,z)\frac{1}{D(u)}u\,du, \tag{3a}$$

where $u=\mu c_1/|\omega|$, μ is the spatial frequency and ω is the temporal frequency,

$$N(\omega,u,z)=\exp\left(i\,\mathrm{sgn}(\omega)\frac{\omega}{c_1}(h\sqrt{1-u^2}+z\sqrt{n^2-u^2})\right),$$
$$D(u)=m\sqrt{1-u^2}+\sqrt{n^2-u^2} \tag{3b}$$

with the determination defined by

$\sqrt{n^2-u^2}$ define as $i\,\mathrm{sgn}(\omega)\sqrt{|n^2-u^2|}$, for $u>n$,

and

$\sqrt{1-u^2}$ define as $i\,\mathrm{sgn}(\omega)\sqrt{|1-u^2|}$, for $u>1$.

(J_0 is the Bessel function of order zero),

We can remark that the variable u appears naturally in the harmonic case, as the sine of the incidence angle θ of a plane wave ($u=\sin\theta$).[11] (Decomposition of the incident spherical monochromatic wave in plane waves.) Here the approach is different, due to the dependence of u on the spatial frequency μ and on the temporal frequency ω [cf. (3b)].

However, the integral over the variable u can still be decomposed into three contributions that correspond to the branch points in the integrand:

$$\hat{\Psi}=\underset{u<n}{\hat{\Psi}^1}+\underset{n<u<1}{\hat{\Psi}^2}+\underset{u>1}{\hat{\Psi}^3}.$$

The first contribution defined by the interval $[0,n]$ is the "geometric" contribution. The second one corresponding to values of u between $[n,1]$ is the called "lateral" or "surface" contribution, in analogy with the terminology of the harmonic case. The last one, corresponding to values u $[1,\infty]$, is the "evanescent" contribution.

We should notice that the second contribution arises in the harmonic case from an additional integral around the branch point n, whereas it is given here as the contribution of the interval $n<u<1$ to the integral over the variable u.

II. DECOMPOSITION OF THE GREEN'S FUNCTION

Our aim is to calculate separately each contribution and to study its dependence on the properties of the source and on the position of the observation point. Consequently we shall study partial Green's functions for the direct problem, i.e., the case of an impulse point source.

If we assume that the source signal is an impulse, that is, $\hat{F}(\omega)=C^{st}$, expression (3) corresponds to the Green's function in Fourier–Hankel space:

$$G^j(r,z,t)=\frac{i}{c_1\pi}\int_{\omega=0}^{\infty}e^{i\omega t}\omega\left[\int_{u=u^j_{\min}}^{u=u^j_{\max}}\frac{e^{iN(u,\omega,z)}}{m\sqrt{1-u^2}+\sqrt{n^2-u^2}}\times J_0\left(\frac{u\omega}{r}\right)u\,du\right]d\omega. \tag{4}$$

Since the potential and the source satisfy the Hermitian symmetry [i.e., $\hat{\Psi}(r,z,\omega)=\hat{\Psi}(r,z,-\omega)$], it is not necessary to define the Green's function for values of $\omega<0$. A real and causal solution can be obtained by taking into account the hermiticity and analyticity of the potentials. We consider here complex solutions, so as to study the modulus and phase of each contribution.

With the help of an inverse Fourier transform over the time variable, we can obtain an expression of the various contributions at any point of space and time. The expression contains, however, a double integral. Since the integrals over two variables (u and ω) are independent, we can change the order of integration. A first evaluation of the integral over ω[31] allows us to reduce the calculation of the propagator to the evaluation of a one-dimensional integral over the variable u.

We wish to emphasize the calculation of the propagator associated with "surface" contributions for large radial distances. These contributions—often neglected in the case of a fluid–fluid interface—are important in the study of an inverse problem.[32,33]

A. "Geometric" contribution

Let us define

$$\beta=t-\frac{\sqrt{1-u^2}}{c_1}h-\frac{\sqrt{n^2-u^2}}{c_1}z \quad\text{and}\quad \alpha=\frac{ur}{c_1}.$$

From expressions (3) and (4), using Ref. 31, we obtain

$$G^1(r,z,t)=\frac{-1}{c_1\pi}\int_{u=0}^{n}\frac{u}{m\sqrt{1-u^2}+\sqrt{n^2-u^2}}\times\left(\frac{\partial}{\partial\beta}\int_{\omega=0}^{\infty}e^{-i\omega\beta}J_0(\omega\alpha)d\omega\right)du.$$

We can derive the expression in the sense of distributions (cf. Appendix A):

$$\langle G^1,\phi\rangle=\frac{-1}{c_1\pi}\int_{u=0}^{n}\frac{u}{m\sqrt{1-u^2}+\sqrt{n^2-u^2}}\times[\langle I_+,\phi\rangle H(\alpha-\beta)+i\langle I_-,\phi\rangle H(\beta-\alpha)]du. \tag{5}$$

Here, the notation $\langle\ ,\ \rangle$ represents the evaluation of a functional f by a test function ϕ, i.e., formally $\langle f,\phi\rangle=\int f(x)\phi(x)dx$, and H is the Heaviside function:

$$\langle I_+,\phi\rangle=-\frac{1}{2}\left(\frac{(\alpha+\beta)^{-3/2}}{\sqrt{\alpha-\beta}}+\frac{1}{\sqrt{\alpha+\beta}}\times\int_0^{\infty}[\phi(x)-\phi(0)]x^{-3/2}dx\right),\quad \alpha<\beta,$$

$$\langle I_-,\phi\rangle=-\frac{i}{2}\left(\frac{(\alpha+\beta)^{-3/2}}{\sqrt{\beta-\alpha}}+\frac{1}{\sqrt{\alpha+\beta}}\right.$$
$$\left.\times\int_0^\infty[\phi(-x)-\phi(0)]x^{-3/2}dx\right),\quad \alpha>\beta.$$

The case where the function $\beta-\alpha$ is zero corresponds to the arrival of the wave front of the "geometric" contribution.[11,13] Here, this means it corresponds to the passage of a δ function at the observation point. Asymptotically, the function $\beta-\alpha$ represents the phase associated to the "geometric" contribution. Let us denote by t_{geo} the time associated with the arrival of the wave front at an arbitrary observation point (r,z). The expression for this point is given by a study of the function $f(u)$:

$$f(u)=\beta-\alpha=0\Leftrightarrow t=\tau(u)=\frac{\sqrt{1-u^2}}{c_1}h+\frac{\sqrt{n^2-u^2}}{c_1}z+\frac{ur}{c_1}.$$

This function has an extremum at $r=hu_0/\sqrt{1-u_0^2}+zu_0/\sqrt{n^2-u_0^2}$. The value of $\tau(u)$ at that point is such that:

$$\tau(u_0(r))=\frac{h}{c_1\sqrt{1-u_0^2}}+\frac{zn}{c_2\sqrt{n^2-u_0^2}}.$$

We find here the trajectory corresponding to Fermat's principle in accordance with the results obtained in the harmonic case with the help of the method of stationary phase $[t_{geo}=\tau(u_0)]$.

One can remark that for $u=0$, $\tau(u)=h/c_1+z/c_2=\tau_0$. This value corresponds to the minimum time that the wave can take in order to arrive at the point $(r=0,z)$. We are now in the situation where the point of the observation is directly under the source.

If $u=n$, $\tau(u)=\sqrt{1-n^2/c_1}\,h+r/c_2=t_1$. This time corresponds to a wave arriving at a critical angle and verifying Fermat's principle in analogy with the results obtained in the harmonic case.

B. "Surface" contribution

The "lateral" contribution that we shall calculate numerically can be written as:

$$G^2(r,z,t)=\frac{-1}{c_1\pi}\int_{u=n}^1\frac{u[\alpha^2-(c+id)^2]^{-3/2}(c+id)}{m\sqrt{1-u^2}+i\sqrt{u^2-n^2}}du, \tag{6}$$

where

$$\beta'=c+id=t-\frac{\sqrt{1-u^2}}{c_1}h+i\left(\frac{\sqrt{u^2-n^2}}{c_1}z\right)$$

and

$$\alpha=\frac{ur}{c_1}.$$

This function does not have singularities. Indeed we always have $\alpha-(c+id)\neq 0$. The arrival time of the wave front associated with the "lateral" contribution is obtained through the study of the function $\alpha-\mathrm{Re}[c+id]=0$. That is, $\tau(u)=ur/c_1+(\sqrt{1-u^2/c_1})h$.

This function has an extremum at $r=hu_0/\sqrt{1-u_0^2}$. At this point one has $\tau(u_0)=hu_0/c_1\sqrt{1-u_0^2}$. We find, in accordance with the results obtained by the saddle point method,[1,11] a distance corresponding to the direct path of a plane wave at the interface. Let t_2 be the time corresponding to this path:

$$t_2=\frac{hu_0}{c_1\sqrt{1-u_0^2}}=\frac{\sqrt{h^2+r^2}}{c_1}.$$

The values of the variable τ at the limits of the integration interval are

$$\tau(n)=t_1=\frac{\sqrt{1-n^2}}{c_1}h+\frac{r}{c_2},\quad \tau(1)=\frac{r}{c_1}.$$

At the lower limit $(u=n)$, we find the same expression t_1 as the one obtained for the "geometric" contribution. The analysis of the "lateral" contribution shows a partial contribution from the "geometric" part. It appears mostly at time t_1. We see, furthermore, that we can make an analogy between the times calculated by stationary phase[1,11] and the times obtained by the study of the function $\tau(u)$. Figure 2(a) represents the modulus of the acoustic potential associated with the surface contribution and Fig. 2(b) represents its phase, for the case where the reduced variable $r/h=2$ and $z/h=0.1$.

On the other hand, even though the sum of the three contributions $G=G^1+G^2+G^3$ verifies the conditions of analyticity, the expressions associated with the partial contributions lose this last property due to the truncation of the integral over the variable u $[u=u(\omega)]$. This explains the "artifact" that appears at time $t_a=t_1-2r/c_2$ (cf. Fig. 2).

The analysis of the "lateral" or "surface" contribution shows a partial contribution of the "geometric" contribution. It is present mostly at the time t_1. We see in addition that we can make an analogy between the times obtained by the method of stationary phase (classical method)[1,11] and the times obtained through the study of the function $\tau(u)$.

C. "Evanescent" or "third" contribution

In this case the integral over the variable ω corresponds to a real and decreasing exponential:

$$G^3(r,z,t)=\frac{1}{c_1\pi}\int_{u=1}^\infty\frac{u}{m\sqrt{u^2-1}+\sqrt{u^2-n^2}}$$
$$\times[(e+it)^2+\alpha^2]^{-3/2}(e+it)du, \tag{7}$$

where

$$\beta''=it+e=it+\frac{\sqrt{u^2-n^2}}{c_1}z+\frac{\sqrt{u^2-1}}{c_1}h\quad\text{and}\quad\alpha=\frac{ur}{c_1}.$$

This function has no singularities and can be numerically computed. We can remark that if we use a classical method (the asymptotic approximation for harmonic case for example) for the field this contribution does not appear. We can see here that it exists, but its influence is

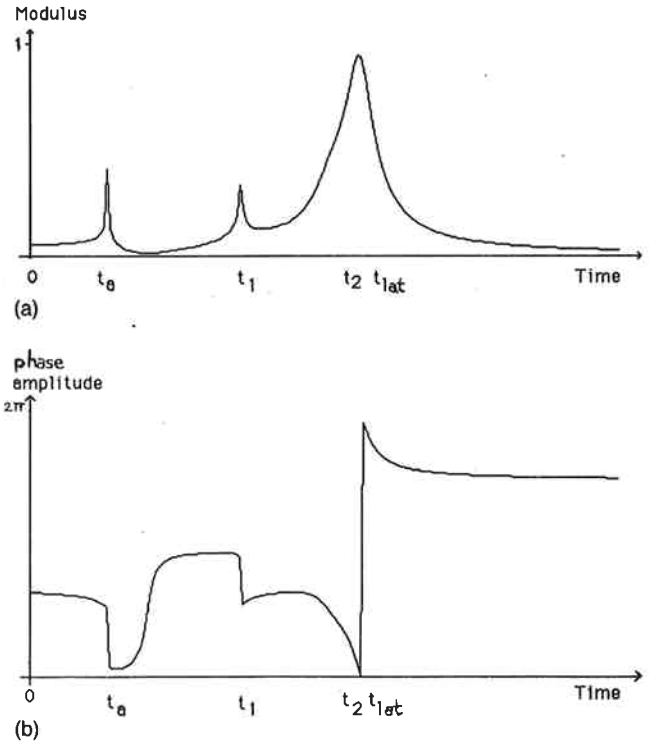

FIG. 2. (a) Modulus of the acoustic potential associated to the "surface" or "lateral" contribution: t_a is the time artifact due to the partition of the field into "geometric," "surface," and "evanescent" contributions (i.e., loss of the analyticity property of the partial potential). This time does not correspond to a physical solution, $t_a=t_1-2r/c_2$ (no-causal solution); t_1,t_2 are the times corresponding (by analogy to a decomposition of a spherical wave into an infinite sum of plane waves) to plane waves arriving under critical incidence following Fermat's principle, and plane waves arriving with an overcritical angle [$t_1 = h(\sqrt{1-n^2}/c_1) + nr/c_1$ and $t_2 = \sqrt{r^2+h^2}/c_1$]; and t_{lat}=time corresponding to the arrival of the "lateral" contribution ($t_{lat}=t_2+zn/c_1$). (b) Phase of the acoustic potential associated to the "surface" or "lateral" contribution: t_a is the time artifact due to the contributions of the field into "geometric," "surface," and "evanescent" contributions (i.e:, loss of the analyticity property of the partial potential). This time does not correspond to a physical solution, $t_a=t_1-2r/c_2$ (no-causal solution); t_1,t_2 are the times corresponding (by analogy to a decomposition of a spherical wave into an infinite sum of plane waves) to plane waves arriving with an undercritical incidence following Fermat's principle, and plane waves arriving with an overcritical angle ($t_1 = h\sqrt{1-n^2}/c_1 + nr/c_1$ and $t_2 = \sqrt{r^2+h^2}/c_1$); and t_{lat} is the time corresponding to the arrival of the "lateral" contribution ($t_{lat}=t_2+zn/c_1$).

negligible. It is very soon attenuated independently of the observation point. This attenuation depends, however, on frequency.

The study of those contributions has shown that they have a different dependencies on time and on frequency. We see that it is appropriate to use a time-frequency method for their characterization. There exist many methods for analyzing a transient signal. We want however to make an exact calculation, while keeping in mind the physics, this leads us to use a linear transform in which the signal is decomposed into a basis of functions that are well localised simultaneously in time and in frequency. The wavelet transform, a time-and-scale method, satisfies these requirements.[24,25] We shall now study, in the time-and-scale space, the behavior of the acoustic pressure field.

III. DECOMPOSITION OF GREEN'S FUNCTION INTO ELEMENTARY WAVELET CONTRIBUTIONS

Assuming that the source emits an impulsive signal, we can decompose the propagator with the help of the wavelet transform into a sum of elementary wavelet contributions.[24–26] This decomposition depends, on one hand, on the properties of the wavelet transform and, on the other hand on the properties of the analyzing wavelet that we choose. Let us assume that the analyzing wavelet $g(t)$ is regular and progressive (cf. Appendix B).

Then the linearity of the transform will allow us to study separately each one of those contributions and to calculate them separately. The wavelet transform of the propagator is more regular than the propagator itself, because of the regularity of the analyzing wavelet.

One obtains a local analysis at $\Delta\omega/\omega=C^{ste}$.[24] This method is consequently different from the classical analysis at $\Delta\omega=C^{st}$ such as the window-Fourier transform, or Gabor transform[25] and well adapted to the detection of discontinuities (e.g., wave front).

One can reconstruct selectively with any desired precision the total transmitted acoustic field. The total field will be obtained by simple summation of the contributions, in distinction to nonlinear methods such as the Wigner–Ville distribution.

Moreover, the isometry property will allow us to interpret the square modulus of the transform as an energy density.[25] We can choose at will the analyzing wavelet while keeping it progressive, which is necessary in the study of propagation phenomena, and this will allow us in addition to have a physical interpretation of the phase of the transform.

Finally this transform is invertible, that is, we can reconstruct the signal starting from the values of its transform. We shall see how this property will be used in the study of the inverse problem.

Let $g(t)$ be the analyzing wavelet, a the dilation parameter, and b the translation parameter. We can write the wavelet transform in Fourier space. The wavelet transform of the transmitted acoustic potential is

$$(L\Phi)(b,a)=\sqrt{a}\int_0^\infty \hat{\Phi}(r,z,\omega)\,\bar{\hat{g}}\,(a\omega)e^{-ib\omega}\,d\omega,$$

$\bar{g}$ is the complex conjugate of g, with our choice of analyzing wavelet (Morlet wavelet):

$$g(t)=\exp(i\omega_0 t)\exp\left(-\frac{t^2}{2\sigma^2}\right)+\text{correction terms},$$

$$\hat{g}(\omega)=\exp\left(-\frac{(\omega-\omega_0)^2}{2}\right)+\text{correction terms},$$

and the condition

$$\hat{g}(\omega)=0, \quad \text{for } \omega\leqslant 0.$$

A. Decomposition of the "geometric" contribution

The role played by the test function $\phi(x)$ in Eq. (5) will be played in (8) by the analyzing function g. The distribution has been replaced by a smooth function of two

variables. The singular nature of the distribution is manifested in the asymptotic behavior of its wavelet transform for small scales ($a \to 0$). This is an advantage in numerical calculations. On the other hand, the asymptotic behavior of the transform (cone pointing towards the singularity) still allows a localization of the wave front.

The expression is, in that case,

$$(LG^1)(b,a)=\frac{i}{c_1}\sqrt{\frac{2a}{\pi}}\int_{u=0}^{n}\frac{u}{m\sqrt{1u^2+\sqrt{n^2u^2}}}\times\left(\int_{\omega=0}^{\infty}\omega\hat{g}(a\omega)e^{i\omega\Phi(u)}J_0(\eta(u))d\omega\right)du. \tag{8}$$

This formula has been numerically evaluated for different positions of the hydrophone.

B. Decomposition of the "surface" contribution

For this particular contribution we have obtained by the use of the expression[31]

$$(LG^2)(b,a)=\frac{-1}{\pi\sqrt{ac_1}}\int_{u=n}^{1}\frac{u}{m\sqrt{1-u^2+i\sqrt{u^2-n^2}}}\times\left[\int g\left(\frac{t-b}{a}\right)[\alpha^2(c+id)^2]^{3/2}\times(c+id)dt\right]du,$$

$$c=t-\frac{\sqrt{1-u^2}}{c_1}h,\quad d=\frac{\sqrt{u^2-n^2}}{c_1}z,\quad \text{and}\quad \alpha=\frac{ur}{c_1}. \tag{9}$$

The time-scale analysis allows us a correct study of the frequency and time behavior of this contribution.

C. Decomposition of the "third" contribution

The expression for this contribution is

$$(LG^3)(b,a)=\frac{1}{\pi\sqrt{ac_1}}\int_{u=1}^{\infty}\frac{u}{m\sqrt{u^2-1}+\sqrt{u^2-n^2}}\times\left[\int g\left(\frac{t-b}{a}\right)[(e+it)^2+\alpha^2]^{-3/2}\times(e+it)dt\right]du, \tag{10}$$

$$e=\frac{\sqrt{u^2-n^2}}{c_1}z+\frac{\sqrt{u^2-1}}{c_1}h\quad\text{and}\quad\alpha=\frac{ur}{c_1}.$$

Even though this contribution is negligible for the values of the parameters m,n that we will use, we shall take it into account in our numerical evaluations.

IV. NUMERICAL EVALUATION AND INTERPRETATION OF RESULTS

The theoretical study of different contributions that constitute the transmitted field is combined with a numerical study. We calculate numerically each one of the three contributions. We do this exactly, that is, without using asymptotic approximations. This evaluation can be done separately thanks to the wavelet transform with respect to the analyzing wavelet $g(t)$. Each one of the contributions requires the evaluation of a double integral. The algorithms that we have used are of Romberg's type adapted to the singularities of the integral (algorithm HP[34]). Using the reduced variables $x=r/h$, $y=z/h$, and $\lambda_0=1/h$, in the expressions (8) and (9), we are led to introduce a new variable $\tau_0=h/c_1$. This variable corresponds to the unit time that the wave needs to come from the source to the interface. The new parameters of dilation and translation α and β can then be written as follows:

$$\alpha=\frac{a}{\tau_0},\quad \beta=\frac{b}{\tau_0}\quad\text{with}\quad v=\frac{\omega}{\omega_0},\quad \omega_0=\frac{2\pi}{\tau_0}.$$

The curves of constant modulus and the phase of the wavelet transform are represented as level lines. The level lines of the modulus vary logarithmically with a dynamic range of 32 dB. The levels increase from white to black. The lines of constant phase are linearly coded between $-\pi$ and π. The abscissa is the translation parameter refered to the unit time $\tau_0=h/c_1$.

The ordinate is the dilation parameter divided by this unit time. The signal is analyzed over 6 octaves starting with the dilation parameter 0.15. Each octave is decomposed linearly into five voices.

We now analyze for particular positions of the observation point (hydrophone) the transmitted signal through the interface.

A. Case where the observation point is located under the source

1. "Geometric" contribution (x=0, y=0.2) (Fig. 3)

The emitted signal is an impulse. The analysis of the wavelet transform shows a concentration of energy at the time where the discontinuity of the signal appears. It is at the time $t_0=t_{geo}$. One can see this on the lines of constant modulus, where the modulus is maximum. The analysis of the phase of the transform shows that the lines of constant phase converge all towards the same time corresponding to the exact arrival time of the "geometric" contribution.

Quantitatively, we have

$$t_{geo}=\frac{h}{c_1}+n\frac{z}{c_1}\Rightarrow\frac{t_{geo}}{\tau_0}=(1+ny)=1.045.$$

We obtain for the representation of the modulus [Fig. 3(a)] and the phase [Fig. 3(b)] of the wavelet transform, the analog of the wavelet transform of an impulse δ. The interface appears transparent to the propagated signal (that is, there is no deformation but only a decrease of the amplitude as $1/R$ and loss of energy by reflection). We find here again, the characteristics of the "geometric" contribution in the harmonic case.

2. "Surface" contribution (x=0, y=0.2) (Fig. 4)

The analysis of the modulus of wavelet transform of the "surface" or "lateral" contribution shows that this con-

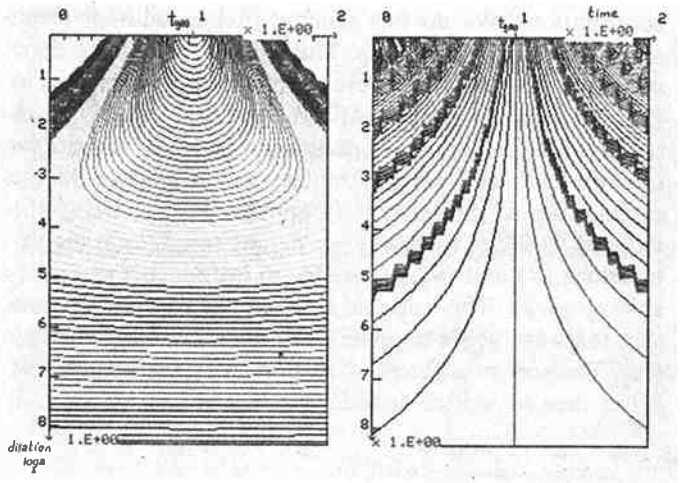

(a) (b)

FIG. 3. (a) Modulus of the wavelet transform of the acoustic potential associated to the "geometric" contribution. The observation point is just under the source at a radial distance $r/h=0$, and at a depth $z/h=0.2$. (b) Phase of the wavelet transform of the acoustic potential associated to the "geometric" contribution at the same observation point ($r/h=0$, $z/h=0.2$).

tribution exists for incidence angles less than the critical angle (contrary to what one is led to believe by a classical study in the harmonic case and stationary phase), but that the energy associated to this contribution is negligible (ratio of 10^{-6}) compared to the "geometric" contribution. Nevertheless, we can calculate for this wave the arrival time in a precise way, and in this case the arrival time is the same as the arrival time of the "geometric" contribution ($t_{\text{lat}} \approx t_{\text{geo}} = 1.045$).

3. "Evanescent" contribution

Independent of the coordinate of the observation point, this contribution is negligible. It has no special concentration of energy. We shall show it for illustration porposes for the value $x=1.5$, $y=0.1$ (Fig 7).

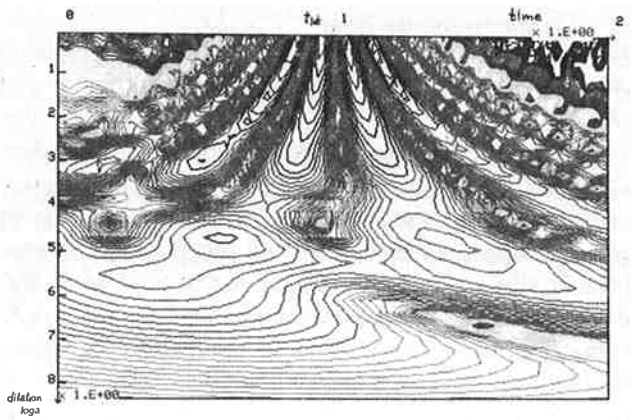

FIG. 4. Modulus of the wavelet transform of the acoustic potential associated to the "surface" contribution. The observation point is just under the source at a radial distance $r/h=0$, and at a depth $z/h=0.2$.

B. Case where the observation point is located at a radial distance larger than the sine of the critical angle ($r/h>0.25$)

We are now in a region where the "surface" contribution is important with respect to the "geometric" contribution (incidence angle greater than the critical angle).

1. "Surface" contribution ($x=r/h=1$, $x=1.5$, and $y=z/h=0.1$) (Fig. 5)

The analysis of the modulus of the wavelet transform allows us to see a very important phenomenon, namely a concentration of energy at small values of the scale parameter for particular times t_1 and t_2 [Fig. 5(a) and (b)]. These times are in agreement with the theoretical study of the "surface" propagator. The "echo" at time t_2 corresponds to the direct trajectory of the wave that arrives under incidence higher than critical at a point M of the interface just under the hydrophone. The time t_1 corresponds to the trajectory of a wave satisfying Fermat's principle. Quantitatively, if $x=r/h=1$, we have to find an energy concentration at times t_1, t_2, t_{lat}, where

$$t_1=\frac{h\sqrt{1-n^2}}{c_1}+\frac{r}{c_2} \Rightarrow \frac{t_1}{\tau_0}=1.28,$$

$$t_2=\frac{\sqrt{r^2+h^2}}{c_1} \Rightarrow \frac{t_2}{\tau_0}=\sqrt{x^2+1}=1.414,$$

$$t_{\text{lat}}=t_2+\frac{z}{c_2} \Rightarrow \frac{t_{\text{lat}}}{\tau_0}=\frac{t_2}{t_0}+yn=1.436.$$

Notice also the artifact time:

$$t_a=\frac{h\sqrt{1-n^2}}{c_1}-\frac{r}{c_2} \Rightarrow \frac{t_a}{\tau_0}=0.747.$$

As we already mentioned, energy concentration at the time t_a corresponds to a loss of analyticity of the spatial solution due to the truncation of the integral over the variable u and consequently over the variable ω. We observe the same phenomenon for the "geometric" contribution (Sec. IV B 2) and in the study of the partial propagator (Sec. II). A summation over the three contributions makes this artifact disappear.[13] These phenomena of echos associated to the times t_1,t_2 will turn out to be important when we study the inverse problem.[32,33] Figure 5(c) represents the modulus of the wavelet transform of the real part of the surface contribution ($r/h=1$, $z/h=0.1$). It corresponds to the pressure measured at a hydrophone. We obtained for $r/h=1.5$:

$$\frac{t_1}{\tau_0}=1.314, \quad \frac{t_2}{\tau_0}=1.807, \quad \frac{t_{\text{lat}}}{\tau_0}=1.829, \quad \text{and} \quad \frac{t_a}{\tau_0}=0.634.$$

2. "Geometric" contribution ($x=r/h=1$ and $x=1.5$, and $y=z/h=0.1$) (Fig. 6)

The analysis of the modulus of the transform of this contribution shows a concentration of energy at some definite times. If the scale parameter is small, the lines of constant phase, where the modulus is maximum converge towards two discontinuities of the signal [the arrival time

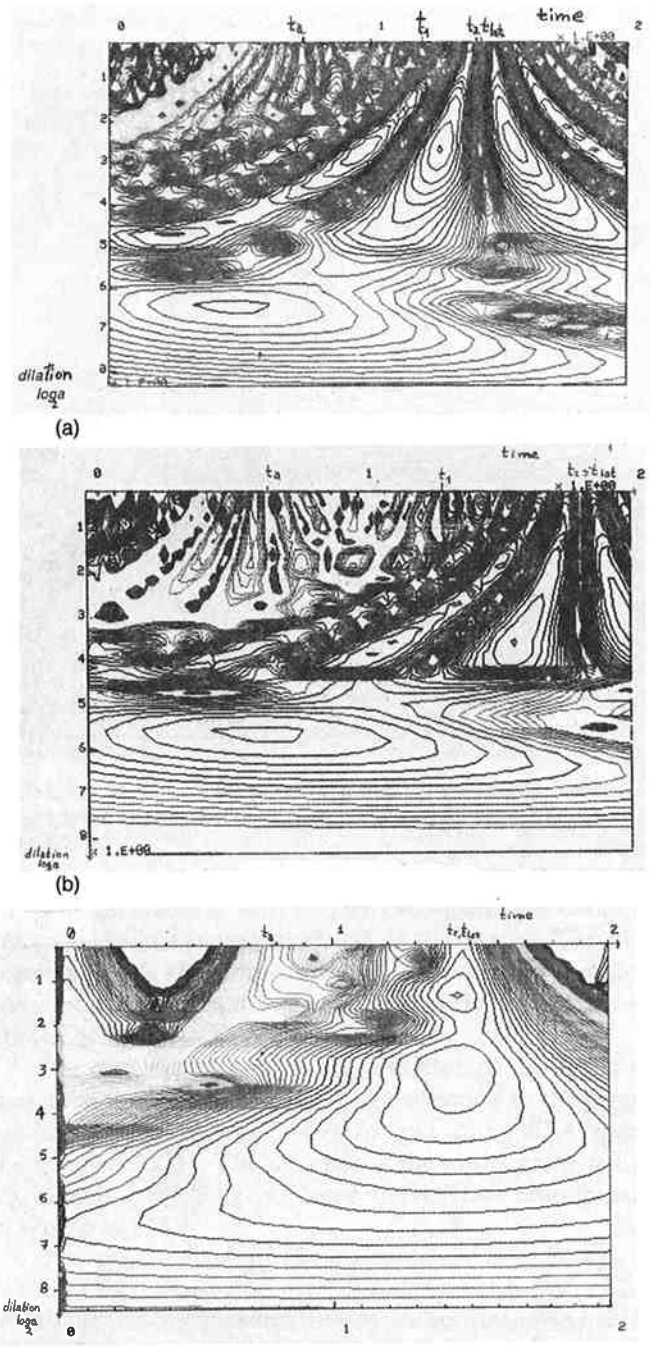

FIG. 5. Modulus of the wavelet transform of the acoustic potential associated to the "surface" contribution. The observation point is located at a radial distance larger than the sine of the critical angle and at the depth $z/h=0.1$. (a) $r/h=1$: the different arrival times are $t_1=1.28$, $t_2=1.414$, $t_{\text{lat}}=1.436$, $t_a=0.747$; (b) $r/h=1.5$, the different arrival times are $t_1=1.314$, $t_2=1.802$, $t_{\text{lat}}=1.829$, $t_a=0.634$; (c) Modulus of the wavelet transform of the real part of the "surface" contribution at the observation point $r/h=1$ (radial distance) and $z/h=0.1$ (depth).

of the "geometric" contribution (t_{geo}) and of an echo (t_1)]. We have a second concentration of energy at the artifact time $t_a \approx 0.634$. Quantitatively we have for $r/h=1$:

$$t_{\text{geo}}=\frac{h}{c_1\sqrt{1-u^2}}+\frac{zn^2}{c_1\sqrt{n^2-u^2}} \Rightarrow \frac{t_{\text{geo}}}{\tau_0}$$

$$=\frac{1}{\sqrt{1-u^2}}+\frac{yn^2}{\sqrt{n^2-u^2}}=1.19,$$

$$t_1=\frac{h\sqrt{1-n^2}}{c_1}+\frac{r}{c_2} \Rightarrow \frac{t_1}{\tau_0}=\sqrt{1-n^2}+xn=1.2,$$

$$t_a=\frac{h\sqrt{1-n^2}}{c_1}-\frac{r}{c_2} \Rightarrow \frac{t_a}{\tau_0}=\sqrt{1-n^2}-xn=0.747.$$

For $r/h=1.5$ we obtained

$$\frac{t_{\text{geo}}}{\tau_0}=1.22, \quad \frac{t_1}{\tau_0}=1.288, \quad \text{and} \quad \frac{t_a}{\tau_0}=0.634.$$

3. "Evanescent" contribution ($x=1.5$, $y=0.1$) (Fig. 7)

Even though this contribution is very soon attenuated and does not correspond to a propagation phenomenon, we shall give here a representation of the modulus and the phase of its wavelet transform.

V. APPLICATION OF WAVELET TRANSFORM: EXPERIMENTAL RESULTS

In order to verify our results we shall compare them to experiment. The chosen example will be a plane air–water interface. Since time is very important here, there are some special precautions to be taken. The experimental signal (that is, a source signal measured at a microphone and a transmitted signal measured at a hydrophone), will be acquired in such a way that synchronism is assured. The time $t=0$ will be given by a fixed reference microphone associated with a pulse generator, which will start the D/A converter. The source signal and the transmitted signal are sampled synchronously and stored in a bichannel (multiplexed) of the D/A converter.

A. Choice of the source

An ideal source that would allow us to put into correspondence the theoretical results with the experimental results would be a perfect impulse (that is a perfectly flat frequency response). Of course such a source does not exist. However this impulse model can be approached with the help of sources that emit very short signals. We have chosen to use a mechanical point source. The generation of the acoustic signal is performed by a percussion system, which acts on an explosive charge (firecracker). The characteristics obtained in such a way allow us to identify the source with an impulse generator in a frequency domain between 500 Hz and 9 kHz. The support in time is of the order of 8×10^{-4} s. The wavelet analysis of the source signal has confirmed those results (Fig. 9).

A preliminary study of the source has allowed us to verify that the generated wave has a behavior compatible with the spherical wave model ($1/R$ behavior).

B. The acquisition setup

The synchronous acquisition of transmitted and of reference signal is performed by the D/A converter with a sampling rate of 10 μs. The time reference is connected to the emission with the help of a pulse generator that starts the acquisition.

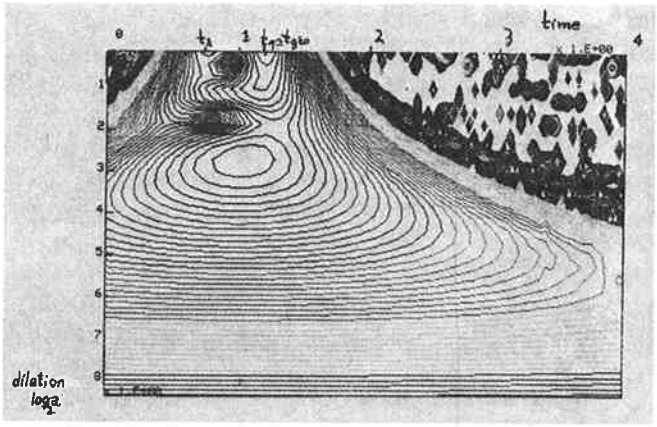

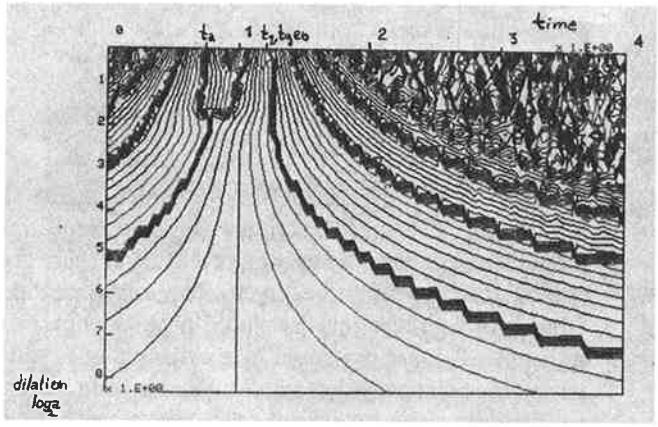

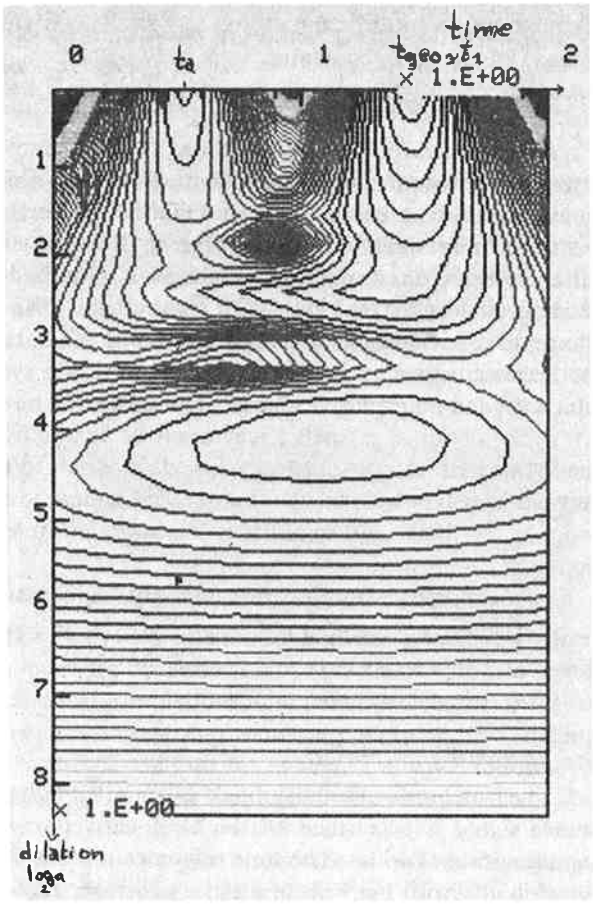

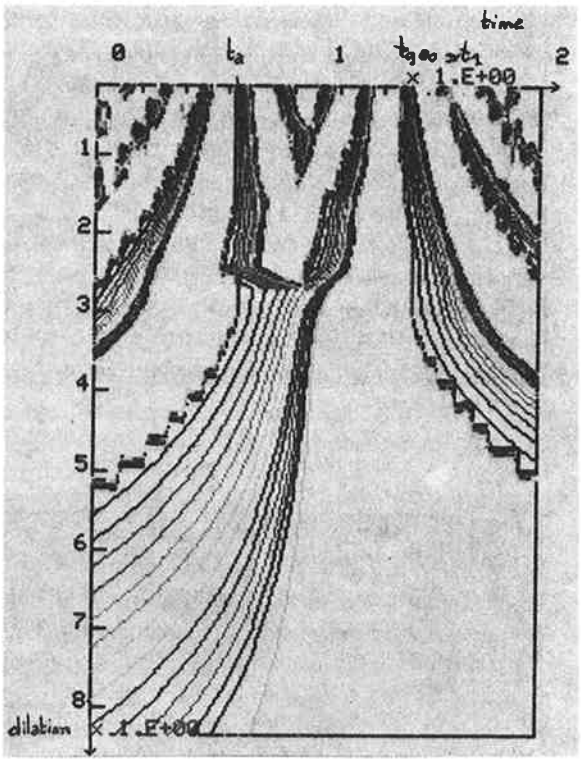

FIG. 6. Wavelet transform of the acoustic potential associated to the "geometric" contribution at a depth $z/h=0.1$ and a radial distance $r/h=1$: (a) modulus and (b) phase. Wavelet transform of the acoustic potential associated to the "geometric" contribution at a depth $z/h=0.1$ and a radial distance $r/h=1.5$: (c) modulus and (d) phase.

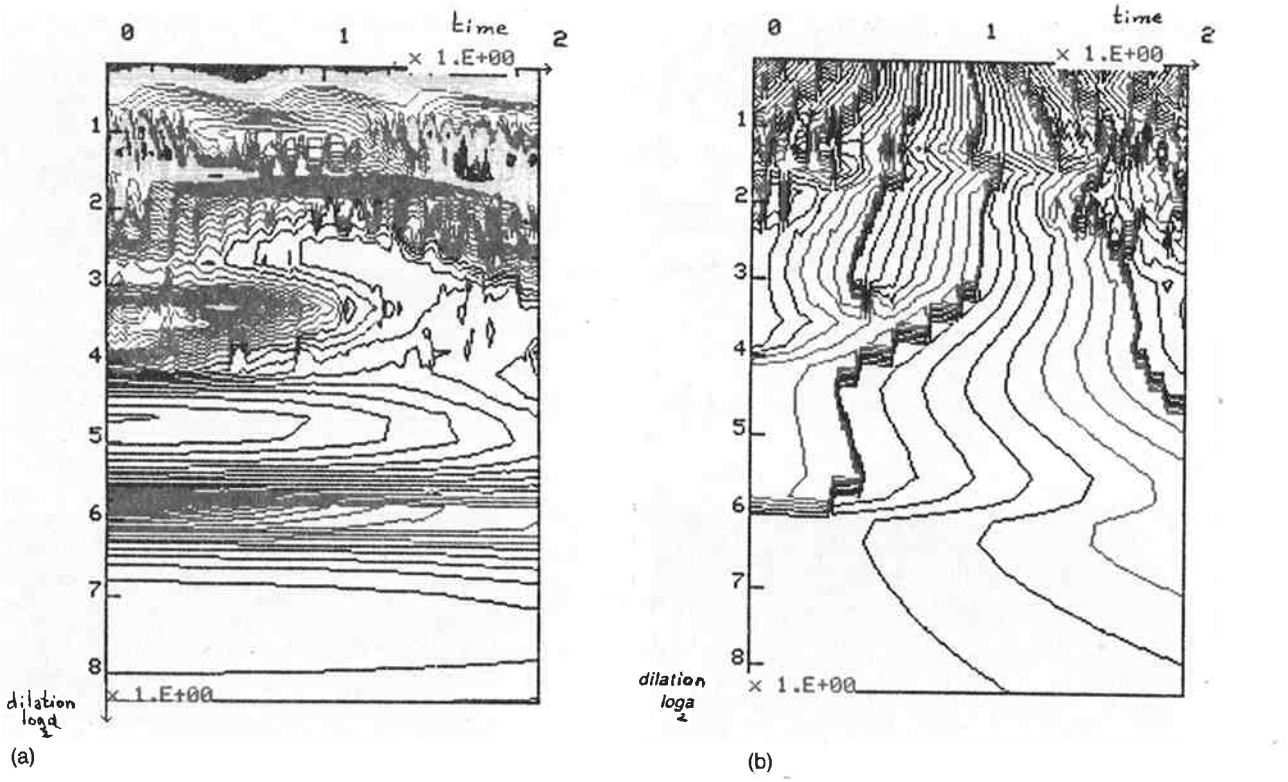

FIG. 7. (a) Modulus of the wavelet transform of the acoustic potential associated to the "evanescent" contribution at the depth 0.1 and radial distance $r/h=1.5$; and (b) phase of the wavelet transform of the acoustic potential associated to the "evanescent" contribution at the depth 0.1 and radial distance $r/h=1.5$.

The generator is activated by the signal received at a microphone in the neighborhood of the source. The numerical signals are then transferred to a computer in order to be treated numerically. The scheme of the experiment is shown in Fig. 8.

For each experiment, the temperature of the media is measured in order to calculate the correction to the propagation velocities ($c_1=344$ m/s and $c_2=1485.4$ m/s, $n=c_1/c_2=0.2322$). The densities of the media are $\rho_1=1.2$ kg/m^3 and $\rho_2=998$ kg/m^3, respectively. Their ratio is then $m=\rho_2/\rho_1=831$.

The preamplifiers of the hydrophones have been adjusted in such a way that the "digitalization" is performed with maximal dynamics. The acquisition was made over 2048 samples corresponding to a duration of 20 ms. This is compatible with the decrease due to the propagation and the duration of the transmitted signal.

C. Experimentation

We analyze here the behavior of the transmitted total pressure field. The source is at 1 m from the water surface. The hydrophone is in a region that corresponds to an incidence angle that is higher than critical ($r=1$ m and $r=1.5$ m, $z=0.1$ m).

1. Analysis of the source signal (Fig. 9)

We have first analyzed the source signal by a wavelet transform performed with respect to analyzing the Morlet wavelet. The analysis has been performed over 6 octaves starting with the scale parameter $a=0.8$, which corresponds to the useful frequency band of the signal. The analyzing wavelet oscillates at a mean frequency of 8130 Hz, for a dilation parameter of 1. Each octave has been decomposed into five voices. The abscissa represents the time in milliseconds and the ordinate is the dilation parameter in logarithmic scale. The graphical representation is the same as the one used in numerical evaluations.

Figure 9(a) represents the modulus of the wavelet transform of the source signal. Although the signal shows some increase in amplitude around 16 kHz (scale parameter around 2), we can consider that it is an impulse signal in the useful frequency band under consideration.

There is a concentration of energy around the time 17 ms corresponding to the arrival time of the impulse signal to the reference microphone.

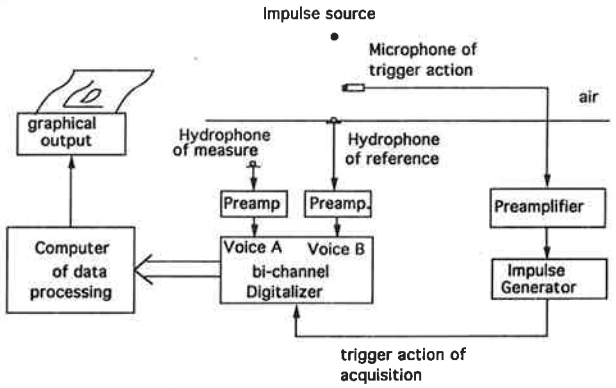

FIG. 8. Scheme of the experiment.

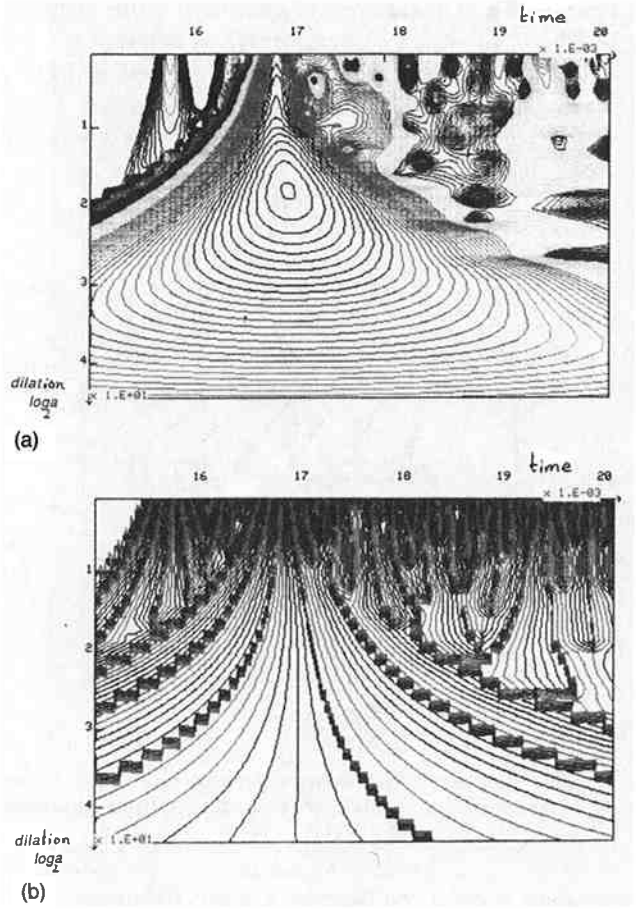

FIG. 9. (a) Modulus of the wavelet transform of the experimental impulse signal (source signal). The analysis has been performed over 6 oct starting with the scale parameter $a=0.8$. For $a=1$, the analyzing wavelet oscillates at mean frequency of 8.130 kHz. (b) Phase of the wavelet transform of the experimental impulse signal (source signal).

We notice—at small scales (high frequencies) and at times earlier than the arrival of the source signal—another impulse of small energy. It corresponds to the recording of the motion of a switch that synchronously activates the measuring instruments. It does not interfere with the analysis of the emitted and transmitted signals. Furthermore, we can see, after the emission of the signal, its reflections on the wall of the room in which the experiment was conducted, mixed with ambient noise.

The phase of the wavelet transform of the emitted signal is presented Fig. 9(b). It can be used to determine with precision the exact arrival time of the signal.

2. Analysis of the transmitted signal (Fig. 10)

The analysis of the modulus of the wavelet transform of the pressure field shows—in agreement with the results of numerical simulations (for small values of the scale parameter)—a concentration of energy at two definite times, corresponding to the arrival of a wave, followed by an "echo" [Fig. 10(a) and (b)]. We can also see echos created by reflections on the walls of the acoustic tank ($r=2$ m). The wavelet transform allows us to separate them from the transmitted signal. They appear in different times and frequencies.

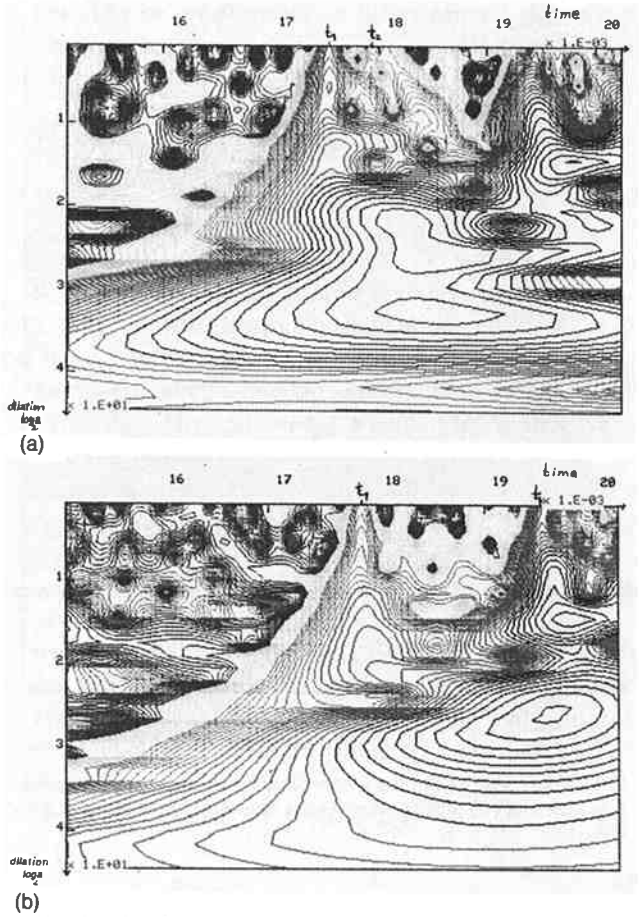

FIG. 10. Modulus of the wavelet transform of the total transmitted signal (experimental acoustic pressure field): (a) $r=1$ m, $z=0.1$ m, $h=1$ m; (b) $r=1.5$ m, $z=0.1$ m, $h=1$ m.

For the observation point located at $r=1$ m, $z=0.1$ m, the theoretical value of these times is

$$t_1=h\frac{\sqrt{1-n^2}}{c_1}+\frac{r}{c_2}=3.5 \text{ ms},$$

$$t_2=\frac{\sqrt{r^2+h^2}}{c_1}=4.1 \text{ ms}\approx t_{\text{lat}} \quad \left(t_{\text{lat}}=t_2+\frac{z}{c_2}=4.18 \text{ ms}\right).$$

That is, with the experimental values calculated from the moment of the beginning of the source signal (14 ms):

$$t_1=17.5 \text{ ms}, \quad t_2=18.1 \text{ ms}\approx t_{\text{lat}} \quad (t_{\text{lat}}=18.18 \text{ ms}).$$

These values correspond exactly to the obtained experimental values [see Fig. 10(a)]. Similarly, other measures have shown a good correlation between theoretical and experimental results.

For the observation point located at $r=1.5$ m, $z=0.1$ m, the theoretical values of the arrival times are

$$t_1=h\frac{\sqrt{1-n^2}}{c_1}+\frac{r}{c_2}=3.83 \text{ ms},$$

$$t_2=\frac{\sqrt{r^2+h^2}}{c_1}=5.24 \text{ ms}\approx t_{\text{lat}} \quad \left(t_{\text{lat}}=t_2+\frac{z}{c_2}=5.3 \text{ ms}\right).$$

The theoretical values calculated from the moment of the beginning of the experimental source signal (14 ms) are

$$t_1=17.83 \text{ ms}, \quad t_2=19.24 \text{ ms} \approx t_{\text{lat}}.$$

The experimental values are

$$t_1=17.8 \text{ ms}, \quad t_2=19.4 \text{ ms} \approx t_{\text{lat}}.$$

The value obtained for the time t_1 is in agreement with our calculation but for the arrival time t_2 we observe a relative error of 8%. In this case we have a motion of the maximum of the energy due to the existence of closed reflected echos (ambient noise) [see Fig. 10(b)]. Other measures have shown a good correlation between theoretical and experimental results for a radial distance 1 m $<r<$ 1.5 m.

Nevertheless, the study by wavelet transforms of the transmission of an impulse wave through the interface has shown the appearance of local phenomena of short duration and low energy. These phenomena are due to the inhomogeneity of the media (interface) which creates the "surface" contribution. They turn out to have a fundamental role in the study of the inverse problem.[34,35]

VI. CONCLUSION

This method can be extended to more general situations (the study of surface waves in a scattering problem generated by a two-layered elastic media, or the study of acoustic propagation through a stratified fluid media).

The decomposition of the propagator into its natural components, together with a use of wavelet techniques, allows a precise study of the surface waves in the case of general time-dependent sources.

The study of the direct problem has allowed us to demonstrate the existence, at some scales and for large radial distances from the sources, of a very short transient phenomenon (an "echo"). This phenomenon has been confirmed by experiments. By analogy of the propagator with the reconstruction formula for wavelet transforms, we can establish a reconstruction formula for the time-dependence of the source signal from simultaneous measures of the transmitted pressure along a vertical.[13,32,35]

ACKNOWLEDGMENTS

I wish to thank Mr. G. Corsain for his help in experiment and Mr. C. Gazanhes for his advice. I would like particularly to express my gratitude to Alex Grossmann, for his helpful advice and numerous discussions, and to P. Tchamitchian. This work has been partially supported by the company DIGILOG (Les Milles) and the G.D.R. "ondelettes" of CNRS, France.

APPENDIX A: "GEOMETRIC" CONTRIBUTION

From expressions (3) and (4), we obtain for the geometric contribution:

$$G^1(r,z,t)=\frac{-1}{c_1\pi}\int_{u=0}^{n}\frac{u}{m\sqrt{1-u^2}+\sqrt{n^2-u^2}} \times\left(\frac{\partial}{\partial\beta}\int_{\omega=0}^{\infty}e^{-i\omega\beta}J_0(\omega\alpha)d\omega\right)du, \quad \text{(A1)}$$

where

$$\beta=t-\frac{\sqrt{1-u^2}}{c_1}h-\frac{\sqrt{n^2-u^2}}{c_1}z \quad \text{and} \quad \alpha=\frac{ur}{c_1}.$$

The integral on the variable ω is explicitly known:[31]

$$I^1(\alpha,\beta)=\int_{\omega=0}^{\infty}e^{-i\omega\beta}J_0(\omega a)d\omega$$

$$=\frac{1}{\sqrt{\alpha^2-\beta^2}}, \quad \text{for } \alpha>\beta \text{ with } \beta>0,$$

$$=\frac{i}{\sqrt{\beta^2-\alpha^2}}, \quad \text{for } \alpha<\beta.$$

Let

$$G^1(r,z,t)=\frac{-1}{c_1\pi}\int_{u=0}^{n}\frac{u}{m\sqrt{1-u^2}+\sqrt{n^2-u^2}} \times\frac{d}{d\beta}\left(\frac{H(\alpha-\beta)}{\sqrt{\alpha^2-\beta^2}}+i\frac{H(\beta-\alpha)}{\sqrt{\beta^2-\alpha^2}}\right)du,$$

where H is the Heaviside function. We can write

$$I^1(\alpha,\beta)=\frac{1}{\sqrt{\alpha^2-\beta^2}}=\frac{1}{\sqrt{\alpha+\beta}}\frac{1}{\sqrt{\alpha-\beta}}, \quad \text{with } \alpha>\beta \text{ and } \beta>0.$$

This function presents a singularity for $\beta=\alpha$. Let

$$I_+=\frac{d}{d\beta}I^1(\alpha,\beta)$$

$$=-\frac{1}{2}\left(\frac{1}{(\alpha+\beta)^{3/2}}\frac{1}{\sqrt{\alpha-\beta}} +\frac{1}{(\alpha+\beta)^{1/2}}\frac{d}{d\beta}\frac{1}{[\sqrt{\alpha-\beta}]_+}\right), \quad \text{for } \alpha>\beta$$

and

$$I_-=\frac{d}{d\beta}I^1(\alpha,\beta)$$

$$=-\frac{i}{2}\left(\frac{1}{(\alpha+\beta)^{3/2}}\frac{1}{\sqrt{\beta-\alpha}} +\frac{1}{(\alpha+\beta)^{1/2}}\frac{d}{d\beta}\frac{1}{[\sqrt{\alpha-\beta}]_-}\right), \quad \text{for } \alpha<\beta.$$

We obtain, if we write $X_+=\alpha-\beta$, where $\alpha>\beta$,

$$\left\langle\frac{d}{d\beta}(X_+^{\lambda}),\phi\right\rangle=\int_0^{\infty}[\phi(x)-\phi(0)]1x^{\lambda-1}dx, \quad \text{with } -1<\lambda<0.$$

The notation $\langle , \rangle$ represents the evaluation of a functional f by a test function ϕ, i.e., formally $\langle f,\phi\rangle = \int f(x)\phi(x)dx$.

In this case the convergence is assured for $X_+ = 0$. We deduce a similar relation for $(d/d\beta)(X_-^\lambda)$, if we write $\langle x_-^\lambda, \phi(x)\rangle = \langle x_+^\lambda, \phi(-x)\rangle$:[35]

$$\langle I_+,\phi\rangle = \left\langle \frac{d}{d\beta} I^1(\alpha,\beta),\phi \right\rangle, \quad \text{for } \alpha > \beta,$$

$$\langle I_-,\phi\rangle = \left\langle \frac{d}{d\beta} I^1(\alpha,\beta),\phi \right\rangle, \quad \text{for } \alpha < \beta.$$

Here, $(d/d\beta)\{X_\pm^\lambda\}$ are defined as ordinary functions for $\alpha \neq \beta$. For $\alpha = \beta$, the Dirac distribution δ appears:

$$\langle I_+,\phi\rangle = -\frac{1}{2}\left(\frac{(\alpha+\beta)^{-3/2}}{\sqrt{\alpha-\beta}} + \frac{1}{\sqrt{\alpha+\beta}} \times \int_0^\infty [\phi(x)-\phi(0)]x^{-3/2}dx\right), \quad \alpha < \beta,$$

$$\langle I_-,\phi\rangle = -\frac{i}{2}\left(\frac{(\alpha+\beta)^{-3/2}}{\sqrt{\beta-\alpha}} + \frac{1}{\sqrt{\alpha+\beta}} \times \int_0^\infty [\phi(-x)-\phi(0)]x^{-3/2}dx\right), \quad \alpha > \beta.$$

We obtain finally:

$$\langle G^1,\phi\rangle = \frac{-1}{c_1\pi}\int_{u=0}^{n} \frac{u}{m\sqrt{1-u^2}+\sqrt{n^2-u^2}} \times [\langle I_+,\phi\rangle H(\alpha-\beta) + i\langle I_-,\phi\rangle H(\beta-\alpha)]du. \tag{A2}$$

APPENDIX B: CONTINUOUS WAVELET TRANSFORM

The main difference between this time-scale linear method and the classical time-frequency methods lies in the fact that a time dilation is used instead of a frequency translation. The window in time, defined by the wavelet itself (analyzing function), is then automatically adapted to the scale in which the signal is analyzed. This method is therefore better adapted to the detection of singularities that the other classical linear time-frequency methods, as for example the Gabor's transformation [analysis at $\Delta f = C^{st}$ instead of $\Delta f/f = C^{st}$ (Ref. 25)]. Besides, the artifacts present in the Wigner–Ville distribution (due to its bilinearity) disappear here since the wavelet transform is linear. By the choice of a suitable complex-valued wavelet without spectral components for negative frequencies, we can work with the modulus and the phase of the transform, which carry complementary information.[25,36]

This transformation gives us the decomposition of an arbitrary signal into a sum of elementary contributions of wavelets. These contributions or "windows" all have the same shape and are obtained by dilation (contraction) D^a and translation T^b from an original wavelet (analyzing wavelet).

They form a two-parameter family $g(b,a)(p) = T^b D^{a[g(p)]}$ (p being a space or time variable), where (b,a) belongs to open half-plane $a > 0$.

Let $s(p)$ be an arbitrary one-dimensional signal and $g(p)$ be the analyzing wavelet. The wavelet transform is written as

$$L_s(b,a) = \int s(p) T^b D^a[\bar{g}(p)]dp = a^\alpha \int s(p)\bar{g}\left(\frac{p-b}{a}\right)dp, \quad a \in R^+, \; b \in R.$$

Here, $\bar{g}$ represents the complex conjuguate of g (a depends only on the chosen normalization, i.e., $\alpha = -1/2$ with the L^2 normalization).

There are many possible choices of wavelets $g(p)$. However, they have to satisfy a—not very restrictive—admissibility condition:

$$\int \frac{|\hat{g}(\omega)|^2}{|\omega|} d\omega < \infty, \tag{B1}$$

where $\hat{g}$ is the Fourier transform of g. In practice, this means $\hat{g}(0) = 0$, i.e., g is of zero mean, $\int g(p)dp = 0$.

An admissibility condition is necessary, since it gives rise to a transform that is isometric, in the following sense:

There exists a constant C_g depending only on the wavelet g, such that for every signal $s(p)$ one has

$$\int |s(p)|^2 dp = C_g^{-1}\int\int |S(b,a)|^2 \frac{dbda}{a^2},$$

$$C_g = 2\pi \int \frac{|\hat{g}(\omega)|^2}{|\omega|} d\omega.$$

This expression allows us to define the square modulus of the wavelet transforms, as a density of energy spread in the time-scale half-plane (b,a). In other words, one has conservation of signal energy. Therefore, an inversion formula exists that allows us to reconstitute the signal. It is written as

$$s(p) = \mathrm{Re}\left[C_g^{-1}\int\int S(b,a)a^{-1/2}g\left(\frac{p-b}{a}\right)\frac{da\,db}{a^2}\right],$$

where Re is the real part. This is not the only possible inversion formula, one also has

$$s(p) = \mathrm{Re}\left[K_g^{-1}\int a^{-1/2}S(p,a)\frac{da}{a}\right],$$

where

$$K_g = (2\pi)^{1/2}\int \frac{\hat{g}(\omega)}{|\omega|}d\omega \quad \text{and} \quad K_g \neq 0$$

and where the wavelet is assumed to satisfy

$$\int \frac{\hat{g}(\omega)}{|\omega|}d\omega < \infty \; (\text{and} \neq 0).$$

This formula has the advantage of reconstructing the signal by a one-dimensional integral over the scale parameter.

We should make the following remark: Independently of the choice of the wavelet, the wavelet transform giving rise to exact reconstruction formulas of the signal, all the

information carried by the signal can be found in its wavelet transform. We do not need any "*a priori*" knowledge of the signal in order to apply the transform, since it is a nonparametric method. However, when we want to study some special characteristics of the signal, we shall choose an analyzing wavelet that is appropriate to the phenomenon to be observed.

We can also impose additional restrictions on g, depending on the problem to be solved. We shall require here the wavelet to be a complex-valued wavelet and progressive [$\hat{g}(\omega)=0$ for $\omega<0$], and to be well localized in time and in frequency space. On the one hand, we can work with two complementary pieces of information of the wavelet transform: its modulus and its phase. On the other hand, the progressivity property of the wavelet allows us to define without artifact the precise phase of the wavelet transform. (For instance, for a monochromatic signal, the phase oscillates with the same pulsation of the periodic signal analized.)

The wavelet used here will be of a Morlet type, i.e., a modulated Gaussian:

$$g(p)=\exp(i\omega_0 p)\exp(-p^2/2\sigma).$$

We have seen that the wavelet has to be admissible (B1). Numerically, this will hold if ω_0 is greater than or equal to 5.5.

On the one hand the properties of this wavelet will allow us to calculate the propagator and to analyze the different contributions of the acoustic transmitted pressure. On the other hand, and this is the most important, the linearity of the transform will allow us to study separately the various contributions of the refracted field. The total field is obtained by summation of the contributions. This transformation, applied to wave propagation, allows us to analyze the signal while keeping track of time and frequency characteristics.

[1] E. Gerjuoy, "Refraction of Waves from a Point Source into a Medium of Higher Velocity," Phys. Rev. **73**, 1442–1449 (1948).

[2] L. M. Brekhovskikh, *Waves in Layered Media* (Wiley, New York, 1960), pp. 292–302.

[3] P. Gottlieb, "Sound Source near a Velocity Discontinuity," J. Acoust. Soc. Am. **32**(9), 1117–1122 (1960).

[4] M. S. Weinstein and A. G. Henney, "Wave Solution for Air-to-Water Sound Transmission," J. Acoust. Soc. Am. **37**, 899–905 (1965).

[5] F. S. Grant and in G. F. West, *Interpretation Theory in Applied Geophysics*, International series in the earth sciences (McGraw-Hill, New York, 1965), pp. 164–185.

[6] R. J. Urick, "Noise Signature of an Aircraft in Level Flight over a Hydrophone in the Sea," J. Acoust. Soc. Am. **52**, 993–999 (1972).

[7] J. V. McNicholas, "Lateral wave contribution to the underwater signature of an aircraft," J. Acoust. Soc. Am. **53**, 1755–1756 (1973).

[8] S. M. Candel and C. Crance, "Direct Fourier Synthesis of Wave in Layered Media and The Method of Stationary Phase," J. Sound Vib. **74**(4), 477–498 (1980).

[9] E. K. Westwood, "Complex ray methods for acoustic interaction at a fluid–fluid interface," J. Acoust. Soc. Am. **85**, 1872–1884 (1989).

[10] N. G. Plumpton and C. T. Tindle, "Saddle point analysis of the reflected acoustic field," J. Acoust. Soc. Am. **85**, 1115–1123 (1989).

[11] G. Saracco, "Transmission acoustique à travers le dioptre air-eau," J. Acoust. **1**, 71–80 (1988).

[12] G. Saracco, C. Gazanhes, and J. Léandre, "Etude de la propagation d'ondes sphèriques monochromatiques: Application numèriques et expérimentales dans le cas du dioptre air-eau," Acustica, **73**(1), 21–32 (1991).

[13] G. Saracco, "Propagation acoustique en régime harmonique et transitoire à travers un milieu inhomogène: Méthodes asymptotiques et transformation en ondelettes" thèse de Doctorat de l'U.E.R II—Luminy, Marseille, France (1989).

[14] A. Derem, *Théorie de la Matrice S et Transformation de Sommerfeld-Watson dans la Diffusion Acoustique* (N. Gespa, CEDOCAR Edition, 1986), Sec. VI, pp. 233–240.

[15] A. D. Pierce, "Relation of exact transient solution for a line source near an interface between two fluids to geometrical acoustics," J. Acoust. Soc. Am. **44**, 33–37 (1967).

[16] D. H. Towne, "Pulse Shapes of Spherical Waves Reflected and Refracted at a Plane Interface separating Two Homogeneous Fluids," J. Acoust. Soc. Am. **44**, 65–76 (1968).

[17] D. Casserau, "Nouvelles méthodes et applications de la propagation transitoire dans les milieux fluides et solides, Nouv. thèse, U.E.R. Paris VII, Paris (1988).

[18] C. H. Wilcox, *Sound Propagation in Stratified Fluids* (Springer-Verlag, New York, 1984).

[19] C. L. Pekeris, "Theory of propagation of explosive sound in shallow water," Geol. Soc. Am. Memoir **27** (1948).

[20] L. Cagniard, *Réflexion et réfraction des ondes séismiques progressives* (thèse) (Gauthier-Villars, Paris 1939).

[21] A. T. De Hoop, "A modification of Cagniard's method for solving seismic pulse problems," Appl. Sci. Res. Sec. B **8**, 349–356 (1960).

[22] J. Van Der Hijden, Propagation of Transient Elastic Waves in Stratified Anisotropic Medium," series. in Appl. Math. and Mech. (North-Holland Amsterdam, 1987), pp. 107–166.

[23] G. Cohen and P. Joly, "Fourth-order finite difference schemes for the wave equation in heterogeneous media", Rapport INRIA, Le Chesnay, France (1989).

[24] A. Grossmann and J. Morlet, "Decomposition of Hardy functions into square integrable wavelets of constant shape," Soc. Int. Am. Math., J. Math. Anal. **15**, 723–736 (1984).

[25] *Wavelet, Time-Frequency Methods and Phase Space,* 14–18 December 1987, C.I.R.M.—Luminy, edited by P. Combes, A. Grossmann, and P. Tchamitchian (Springer-Verlag, Berlin, 1989).

[26] A., Grossmann, R. Kronland-Martinet, and J. Morlet, "Reading and understanding continuous wavelet transforms," in *Wavelet, Time-Frequency Methods and Phase Space,* edited by P. Combes, A. Grossmann, and P. Tchamitchian (Springer-Verlag, Berlin, 1989), pp. 2–20.

[27] R. Kronland-Martinet, J. Morlet, and A. Grossmann, "Analysis of sound patterns through wavelet transforms," Int. J. Pattern Recog. Artif. Intell. **1**, 273–302 (1987).

[28] I. Daubechies, "The wavelet transform, time-frequency localization and signal analysis," to appear in I.E.E.E., Inform. Theory (1987).

[29] G. Saracco, A. Grossmann, and P. Tchamitchian, "Use of wavelet transforms in the study of propagation of transient acoustic signals across a plane interface between two homogeneous media," in *Wavelet, Time-Frequency Methods and Phase Space,* edited by P. Combes, A. Grossmann, and P. Tchamitchian (Springer-Verlag, Berlin, 1989), pp. 139–146.

[30] G. Saracco and P. Tchamitchian, "A study of acoustic transmission of transient signal in an inhomogeneous medium with the help of the wavelet transform. Application to an air–water plane interface," in *Electromagnetic and Acoustic scattering. Detection and Inverse Problems* (June 1988), edited by C. Bourelly, P. Chiapetta, and B. Torresani (World-Scientific, Singapore, 1989), pp. 222–241.

[31] H. Bateman, *Table of Integral Transforms* (McGraw-Hill, New York, 1954), Chap. 2, Form. (25), p. 9.

[32] G. Saracco and P. Tchamitchian, "Retrievial of time-dependent source in an acoustic propagation problem," in *Inverse Problems in Action* (Inv. Probl. and Theoret. Imag.), edited by P. Sabatier (Springer-Verlag, Berlin, 1990), pp. 207–211.

[33] G. Saracco, P. Tchamitchian, and C. Gazanhes, "Transmission à travers un dioptre et reconstruction de la source," in *1^er Congrès C.F.A.* edited by P. Filippi and M. Zakharia (Les Editions de Physiques, Les Ullis, France, 1990), Vol. 51, No. 2, pp. 1049–1052.

[34] P. M. Dew and K. R. James, *Introduction to Numerical Computation in Pascal* (MacMillan, London, 1983).

[35] I. M. Guelfand and G. E. Chilov, *Les Distributions*, traduit par Rideau (Collect. Universt. de Math., Dunod, Paris, 1962).

[36] *Wavelet and Application,* May 1989, CIRM—Luminy, edited by Y. Meyer and T. Paul (Masson–Springer, Paris, 1991), Research Notes in Applied Math. Series.